

Title	Effect of Singularity in Stress Field on Optimum Shape of Ceramics/Metal Joint(Mechanics, Strength & Structural Design)
Author(s)	Murakawa, Hidekazu; Ueda, Yukio
Citation	Transactions of JWRI. 1991, 20(1), p. 109-116
Version Type	VoR
URL	https://doi.org/10.18910/9007
rights	
Note	

Osaka University Knowledge Archive : OUKA

<https://ir.library.osaka-u.ac.jp/>

Osaka University

Effect of Singularity in Stress Field on Optimum Shape of Ceramics/Metal Joint†

Hidekazu MURAKAWA* and Yukio UEDA**

Abstract

Due to their brittleness and poor machinability, ceramics are used in the form of composite structure with metals. However, stress concentration occurs in the region near the edge of interface between the ceramics and the metal. Such high stress may cause cracking of ceramics under thermal loads and reduce the reliability under external loads. In general, the stress concentration greatly depends on the geometry or the shape of the joint.

The authors have proposed a shape optimization procedure based on the reliability estimation and demonstrated the possibility of reducing the failure probability through controlling the shape of the joint in the previous report. However, the stress field near the edge of the interface exhibits a singularity. It is also known that the strength of singularity changes with the geometry of the joint. The relation between the singularity and the failure probability and that between the strength of singularity and the optimum shape were not discussed in the previous report. Thus, these points are focused in this report. Further, the primary factor which is the most effective to reduce the failure probability is investigated.

KEY WORDS: (Shape Optimization) (Optimum Design) (Reliability) (Ceramics) (Metal) (Joint) (Singularity) (Finite Element Method)

1. Introduction

Though new-ceramics have a great potential in various engineering applications, most of them are brittle and poor in machinability. These drawbacks are overcome by introducing composite structure consisting of ceramics and metal. In most cases, ceramics and metal are joined at elevated temperature by methods such as brazing or diffusion bonding. Due to the large difference in thermal expansion coefficients of the two materials, significant magnitude of residual stress is produced during the cooling process after joining¹⁾. Such residual stress created at the bonding region may cause cracking or reduce the bonding strength. Thus, it is desirable to minimize the size of the residual stress and various techniques are developed for this purpose. One such technique is to introduce an interlayer²⁾. Another possible technique is to reduce stress by controlling the shape of the bonding zone³⁾.

The authors treated the problem of reducing the residual stress through shape control as an optimum design problem and developed a numerical method to automatically determine the optimum shape for the given conditions⁴⁾. In this method, the shape is optimized so that the failure probability becomes minimum. The failure probability is

estimated based on the weakest link model hypothesis.

As it is known, the stress field at the edge of the interface has a singularity and its strength changes with the geometry of the joint⁵⁾. This suggests a close relation among the geometry of the joint, singularity of stress field and optimum shape. However, the problem was not discussed from such an aspect. Thus, in the present research, a serial computation in which the geometry of the joint is parametrically changed is conducted to clarify these relations. Based on the results obtained from these computations, the primary factor which is the most effective to reduce the failure probability is investigated.

2. Shape Optimization Method

2.1 Failure probability

As one of the methods to evaluate the strength of brittle materials such as ceramics, methods based on the weakest link hypothesis and the statistics have been proposed⁶⁾. According to this method, the failure probability P_f can be estimated as,

$$P_f = 1 - \exp\{-\int (\sigma/\sigma_0)^m Y(\sigma, 0) dv\} \quad (1)$$

$$\approx 1 - \exp\{-\sum_j \nabla_j (\sigma_j/\sigma_0)^m Y(\sigma_j, 0)\}$$

† Received on May 7, 1991

* Associate Professor

** Professor

where, σ_j and V_j are the maximum principal stress and the volume of the j -th element in FEM analysis. In the above equation, σ_0 and m are the parameters of weibull distribution which are given as material constants and $Y(\sigma_j, 0)$ is the heaviside step function.

2.2 Constraining condition

In case of practical engineering problems, there are certain restrictions so that the product can be machined or produced and fulfill the required function. The shape of the product is also subjected to various constraints. As one of the geometrical constraints, the arc length is assumed to be constant and the optimum shape is sought under this condition. In other words, when the original arc length is L_0 , the arc length of the optimum shape is kept αL_0 , where α is a given constant and referred to as arc length factor. This constraint condition can be written as,

$$L = \alpha L_0 \quad (2)$$

2.3 Optimization problem and objective function

The optimization problem can be stated that, to determine the shape for which the objective function W , which is the failure probability P_f in this case, is minimized under the given constraint condition, i. e.

$$W = P_f \Rightarrow \min \quad (3)$$

with satisfying Eq. (2).

By introducing the Lagrange multiplier λ , an objective function W^* in which the constraining condition is embedded is derived and it is shown to be,

$$W^*(a_i, \lambda) = 1 - \exp\left[-\sum_j V_j \left\{\frac{\sigma_j(a_i)}{\sigma_{01}}\right\}^m\right] - \lambda \{L(a_i) - \alpha L_0\} \quad (4)$$

where, a_i are the design parameters which determines the geometry of the joint. The optimum shape satisfying the constraint can be obtained by simply minimizing the objective function W^* . The detailed numerical procedures for optimization are presented in the reference⁴.

3. Example of Shape Optimization

3.1 Example model

Numerical results of optimization reported in the previous paper are cited here to give the general idea. The model for the example problems is shown in Fig. 1. It consists of ceramics (Al_2O_3) and metal (Cu) parts with the same size. Their height and the diameter are 10 mm and 20 mm, respectively. It is assumed that the variations of material constants with temperature can be neglected and the values at room temperature are used. Table 1 shows the Young's

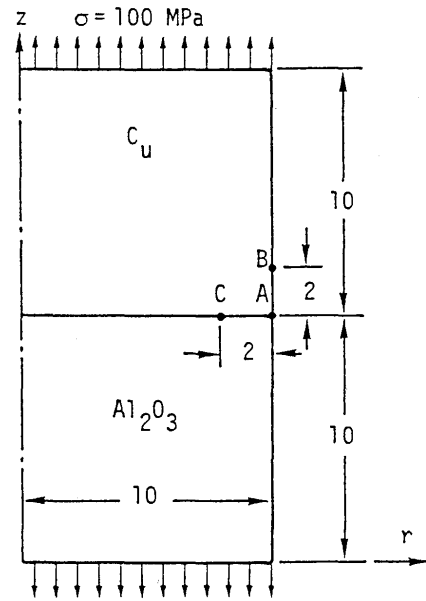


Fig. 1 Example model and region to be modified.

Table 1 Mechanical properties of materials.

	Al_2O_3	Cu
Young's modulus (GPa)	370	130
Poisson's ratio	0.25	0.3
Thermal expansion coef. (1/K)	7.9×10^{-6}	17.7×10^{-6}

moduli, Poisson's ratios and thermal expansion coefficients for the two materials.

The parameters of Weibull distribution which determines the failure probability of the ceramic part, are assumed to be,

$$\sigma_0 = 500 \text{ MPa}, m = 15$$

The above assumed values are not measured ones. They are arbitrarily assumed fictitious values.

3.2 Condition of optimization

The shapes are optimized under the conditions which are given as the combination of the following loading conditions and the constraint conditions on the part of the boundary to be modified.

loading condition

- (1) uniform tensile stress of 100 MPa is acting as an external load
- (2) thermal stress due to temperature drop by $100^\circ C$
- (3) both (1) and (2) are acting simultaneously

boundary to be modified

Side surface of the metal part 2 mm from the interface

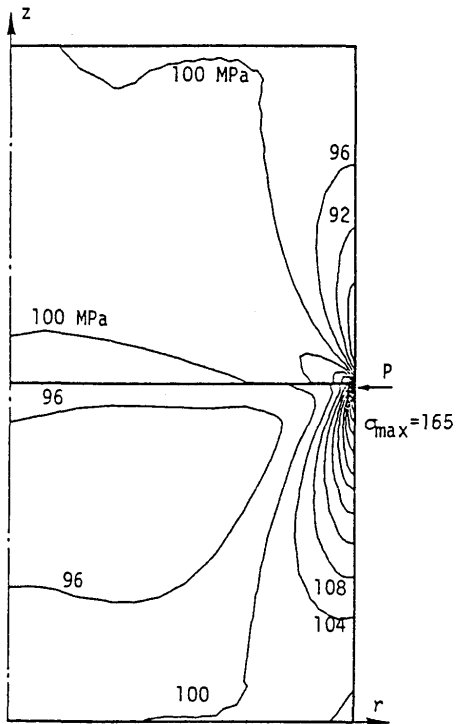


Fig. 2 Distribution of the largest principal stress in the original model under uniform external load.

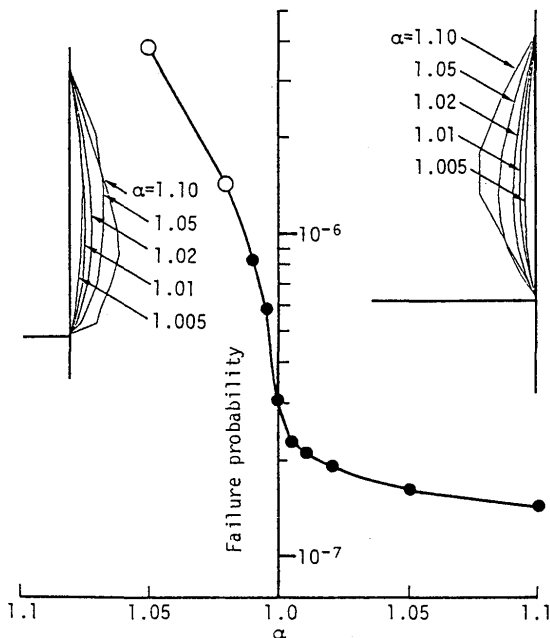


Fig. 3 Optimum shapes and the failure probability under uniform external load.

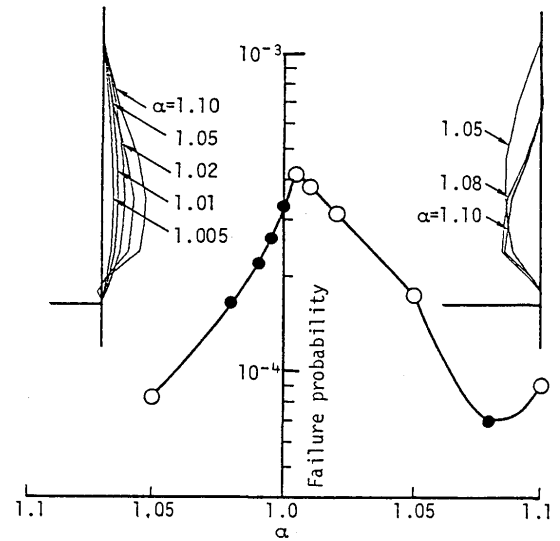


Fig. 4 Optimum shapes and the failure probability under thermal load.

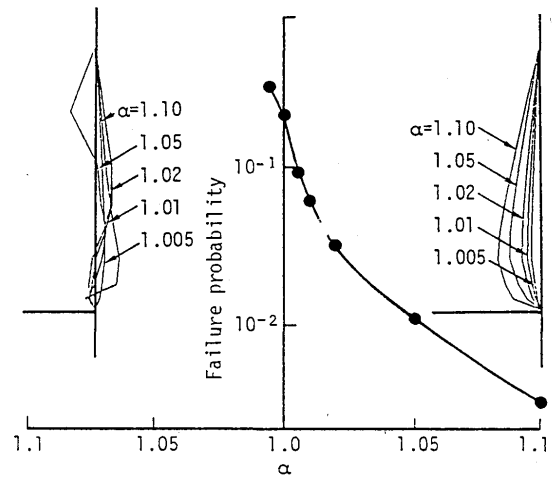


Fig. 5 Optimum shapes and the failure probability under combined load.

(A-B in Fig. 1)

arc length: L

$$L = 1.005 L_0 \sim 1.10 L_0$$

3.3 Numerical result

The distribution of the largest principal stress under external load in the original shape is shown in Fig. 2 as an example. The geometry of the joint is optimized for the three loading cases and the computed optimum shapes and failure probabilities are shown in Figs. 3, 4 and 5. As it has been discussed in the previous report⁴, only the concave shapes are effective to reduce the failure probability in cases under external load and combined load. However both concave and convex forms are effective in case of

thermal load. This suggests that the optimum shape changes with the loading condition.

Though a potential usefulness of the shape optimization has been demonstrated, the following two questions were raised in the previous report.

- (1) Whether the failure probability defined by Eq. (1) takes a fixed value other than 1.0 for stress field with a certain type of singularity?
- (2) What is the primary factor which is effective to reduce the failure probability?

4. Singularity and Failure Probability

It is known that the stress field at the edge of the interface shows a singularity. Thus it is necessary to examine whether the failure probability given by Eq. (1) can be used for such cases. If the failure probability can be computed for a joint between dissimilar materials, the value computed by FEM should converge to a fixed value as the size of elements becomes small.

To study the effect of finite element mesh division on the computed failure probability, a simple automatic mesh generation method is used. In this method, the domains for ceramics and metal are divided into $n \times n$ elements. The size of the element varies in arithmetical series. Let S_{\min} and S_{\max} are the lengths of the smallest and the largest elements, the length of each element S_i can be given by,

$$S_i = S_{\min} + (i-1)\Delta s \quad (5)$$

where

$$\Delta s = \frac{2(\beta-1)}{(\beta+1)} \frac{R}{n(n-1)}$$

$$S_{\min} = \frac{2}{(\beta+1)} \frac{R}{n}, \quad S_{\max} = \frac{2\beta}{(\beta+1)} \frac{R}{n}$$

R is the radius of the specimen and β is a parameter defined as

$$\beta = S_{\max}/S_{\min}$$

Thus, the Finite Element mesh division can be automatically generated if the number of division n and the parameter β are given.

The effect of parameter β on the computed failure probability P_f and the maximum principal stress is studied for three different load conditions. The number of division n is kept as 18 for all cases and the parameter β is changed from 1.0 to 199.0. The case in which $\beta = 1.0$ corresponds to the uniform mesh. The examples of mesh divisions are shown for $\beta = 1.0$ and 29.77 in Fig. 6. The maximum value of the largest principal stress in the ceramics part σ_{\max} and the failure probability P_f are plotted against the size of the smallest element S_{\min} in Figs. 7 and 8. It is clearly seen that

the maximum value of the largest principal stress increases as S_{\min} becomes small. In contrast to the stress, the failure probability plotted in Fig. 8 shows small variation due to the size of the element when only the external load is acting. This implies that the stress is strongly affected by the element size due to its singularity. While, the failure probability P_f shows small effect from mesh division. However, in case of the thermal load and the combined load, the failure probability seems to converge to 1.0 as the size of the element becomes infinitesimally small.

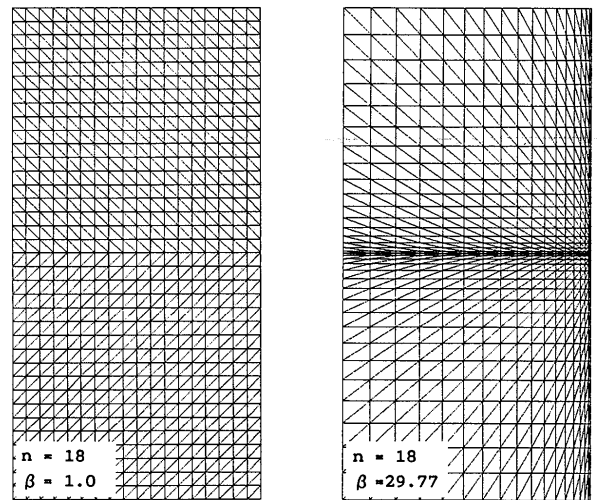


Fig. 6 Mesh division.

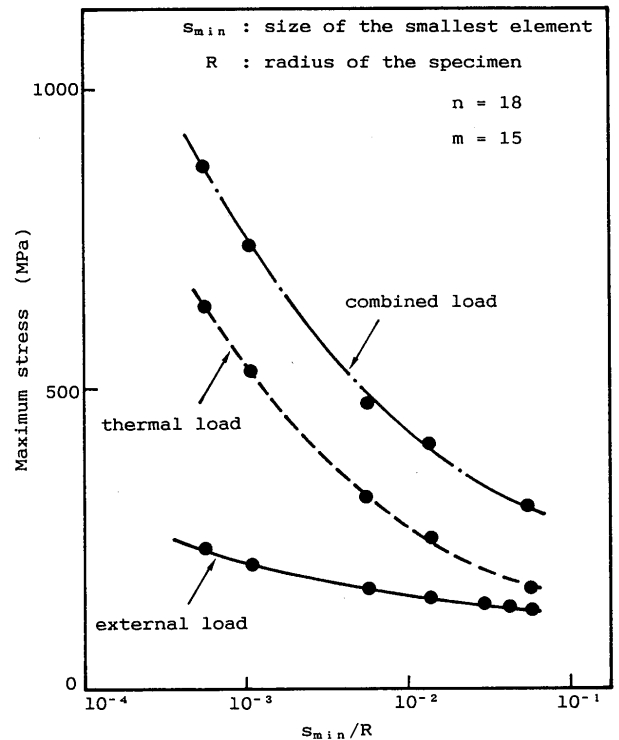


Fig. 7 Effect of element size on the maximum stress in the ceramic part.

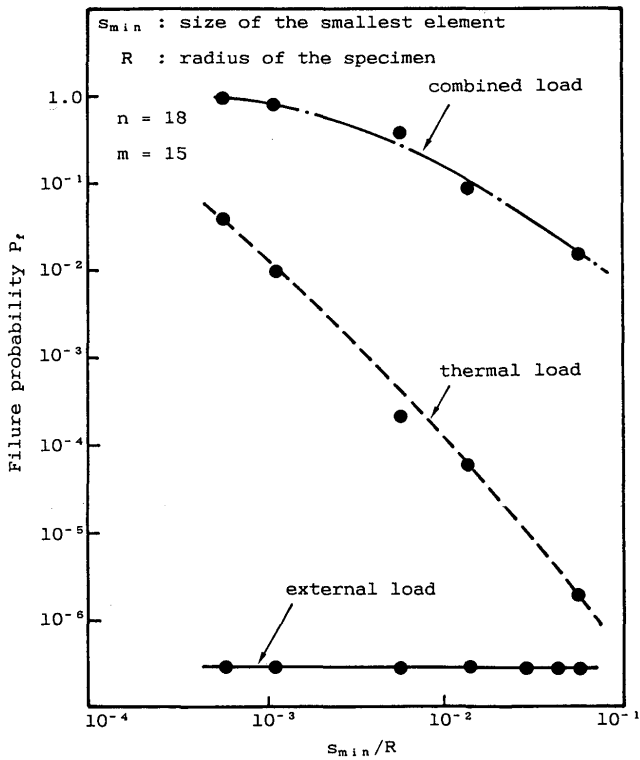


Fig. 8 Effect of element size on the failure probability of the ceramic part.

Further, the effect of the number of division n is examined for cases under external load and thermal load. The effect of material constant m is also examined. In the serial computation, the parameter β is kept as 29.77. The computed failure probabilities are plotted in Figs. 9 and 10. As seen from Fig. 9, the failure probabilities are almost constant for any values of material constant m when external load is acting. In case of thermal load with large m , the failure probability increases with the number of division n .

As far as the numerical results shown in Figs. 9 and 10 are examined, the failure probability under external load may converge to a fixed value when n becomes infinitely large or size of the elements becomes infinitely small. In case of thermal load, it is difficult to see whether the failure probability converges to a value other than 1.0 or not. For a rigorous conclusion, further study is necessary.

5. Effect of Geometrical Factors on Failure Probability.

As discussed in the previous report, the failure probability can be reduced by optimizing the shape of the joint. However, the primary factor which is most effective to reduce the failure probability has not been discussed. Thus,

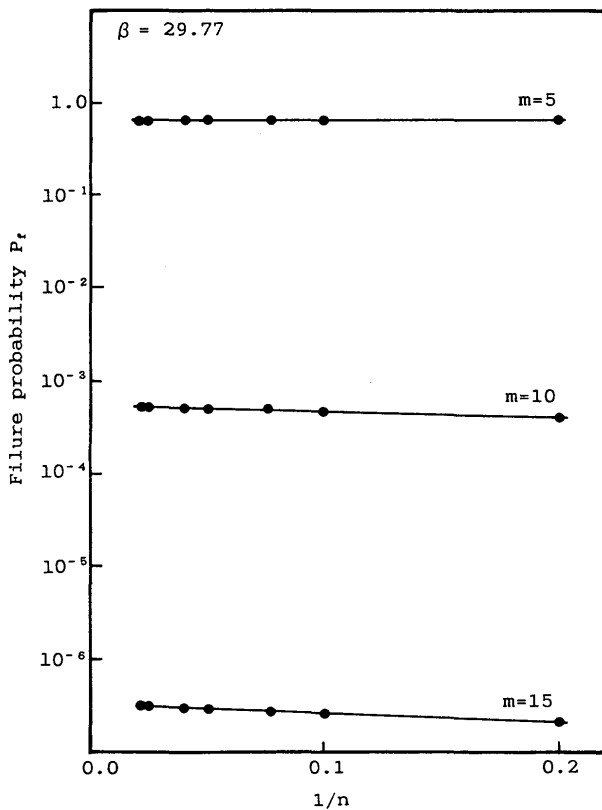


Fig. 9 Effect of the number of division on the failure probability under external load.

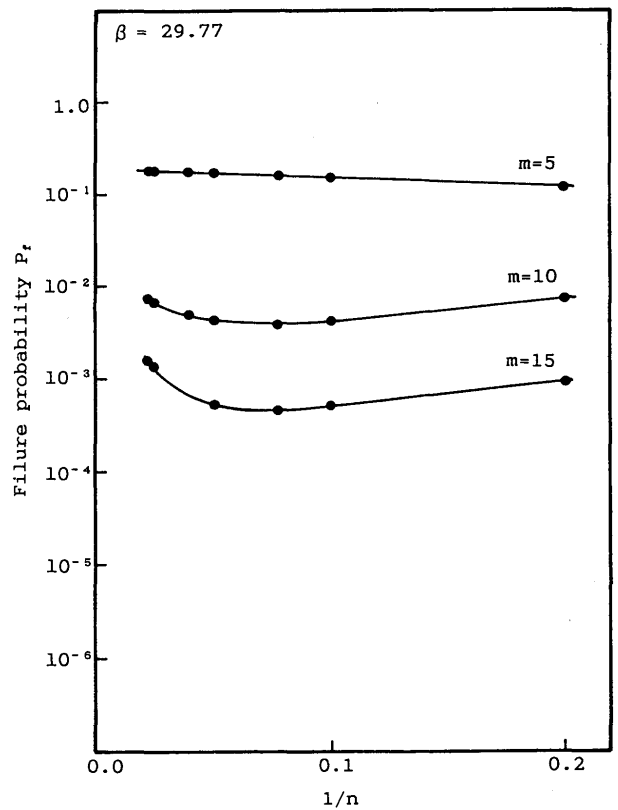


Fig. 10 Effect of the number of division on the failure probability under thermal load.

the effect of various factors on the failure probability is examined in this chapter.

5.1 Strength of singularity in stress field

It is known that certain type of singularity exists at the edge of interface between dissimilar materials. V. L. Hein and F. Erdogan⁹⁾ showed that the strength of singularity changes with the angle between the interface and the side surface of the joint. Based on the figures reported by them, the relation between the strength of the singularity λ and the angle θ is plotted in Fig. 11. The Young's moduli of the two materials are chosen to be $E_1 = 370$ MPa and $E_2 = 130$ MPa, which correspond to Al_2O_3 and C_u in Table 1. However, Poisson's ratios are assumed to be 0.2 for both

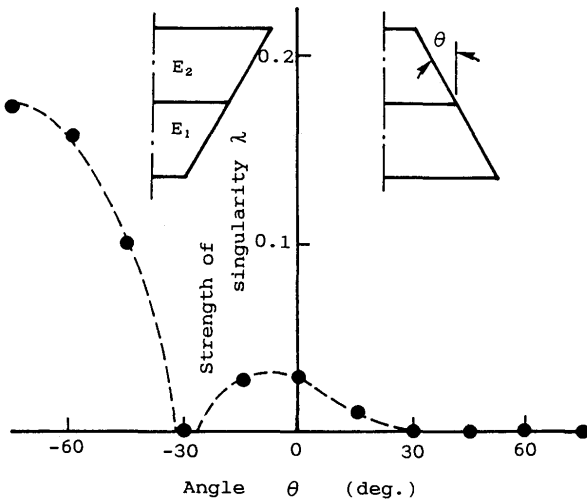


Fig. 11 Relation between the strength of singularity and the angle of interface.

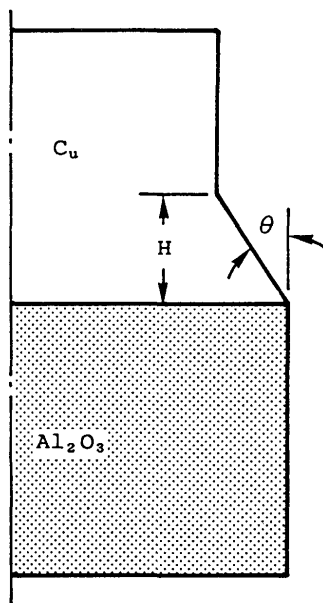


Fig. 12 Geometrical parameters.

materials. In case of such combination of materials, the strength of singularity λ becomes zero when the angle θ is roughly greater than 30° and it is about -30° . From this figure, it may be expected that the failure probability can be reduced by choosing the joint shape which satisfies the above condition on the angle. The fact that the strength of the singularity decreases both in positive and negative values of θ suggests the possibility of reducing the failure probability by both concave and convex shapes as in the case under thermal load shown by Fig. 4.

Though, the strength of singularity λ , which is a function of θ , is an important factor, the failure probability is affected also by other factors as will be discussed in the following sections.

5.2 Effect of edge angle

As the geometrical factors characterizing the shape of the joint, the edge angle θ and the taper length H , which are shown in Fig. 12, are employed. Serial computations, in which θ and H are parametrically changed, are conducted. The relations between the failure probability and the edge angle are shown for the three load conditions discussed earlier. It is clearly seen that relation between the failure probability and the edge angle are quite different among the three load conditions. The variations among the three curves in Fig. 13 explain the result of optimization which are shown in Figs. 3, 4 and 5. This implies that the shape which is effective to reduce the failure probability can not be determined from angle θ alone and the load condition must be also considered. Thus, it is not enough to consider

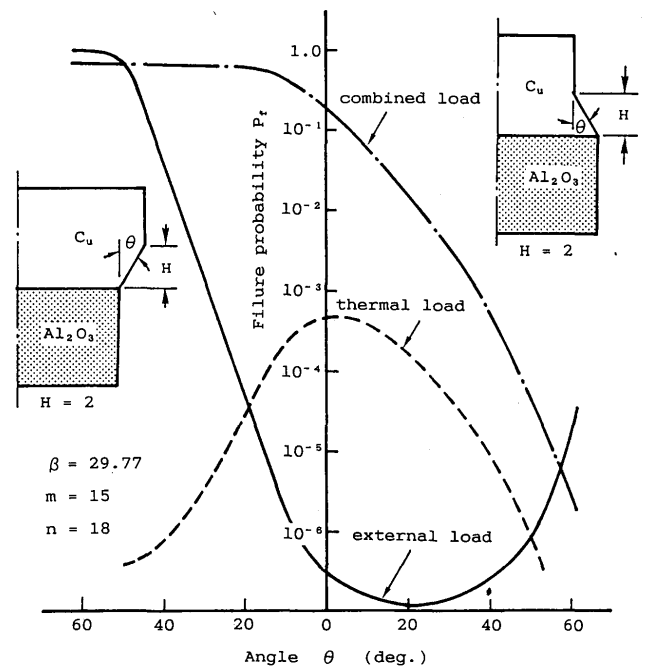


Fig. 13 Effect of edge angle on failure probability.

the strength of singularity λ to reduce the failure probability, because λ is determined by the angle θ and independent on the loading condition.

5.3 Effect of taper length

The effect of the taper length H is examined for the three load conditions. For this computation, the number of mesh division and the parameter β are chosen to be 18 and 29.77, respectively. The computed failure probability is plotted against the taper length H for the two cases in which the edge angles are $\pm 30^\circ$ in Figs. 14 and 15. In case of the thermal and combined loads, the large variation in failure probability is observed for small values of taper length and P_f becomes almost constant when $H > 2$ mm. On the other hand, the failure probability changes even for the large values of the taper length when only the external load is acting. These results implies that the failure is governed by the local stress field very near to the edge of the interface and macroscopic stress has small influence when the thermal load is acting. While, in case of external load, macroscopic stress shows significant influence on the failure probability.

6 Conclusion

The effect of the singularity of stress field on the failure probability and the optimum shape are investigated and the following conclusions are drawn.

- (1) It is shown through the numerical computation that the failure probability converges to a fixed value as the size of element becomes small when only external load is acting on the joint. Thus, the weakest link hypotheses can be applied to evaluate the reliability. However, clear evidence can not be shown for the case in which thermal load is acting.
- (2) The fact that the failure probability under the thermal load can be reduced by both the concave and the convex shapes can be explained by the same relation which holds between the angle of interface and the strength of singularity in stress field.
- (3) If it is assumed that the reliability of ceramics can be estimated based on the weakest link hypothesis, the optimum shape can not be determined by the strength of singularity alone. The other factors such as the lading condition have to be considered.

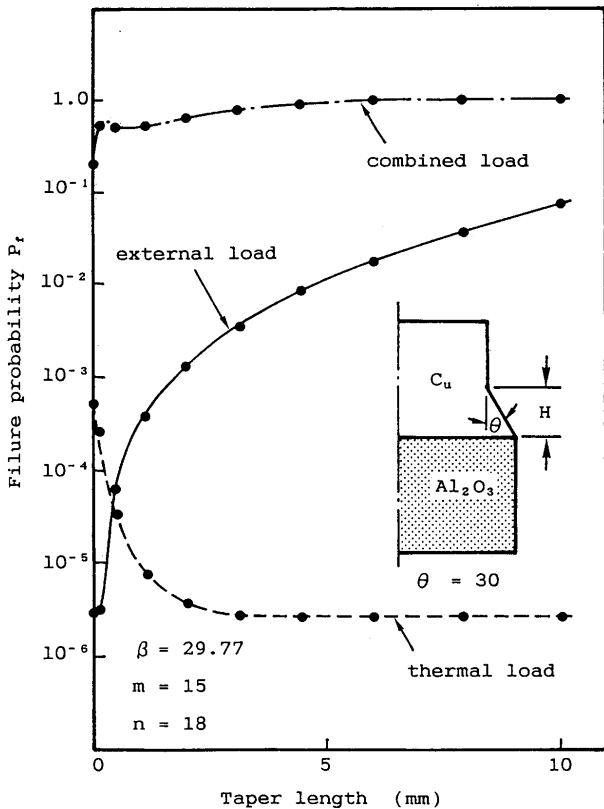


Fig. 14 Effect of the taper length on failure probability (concave type).

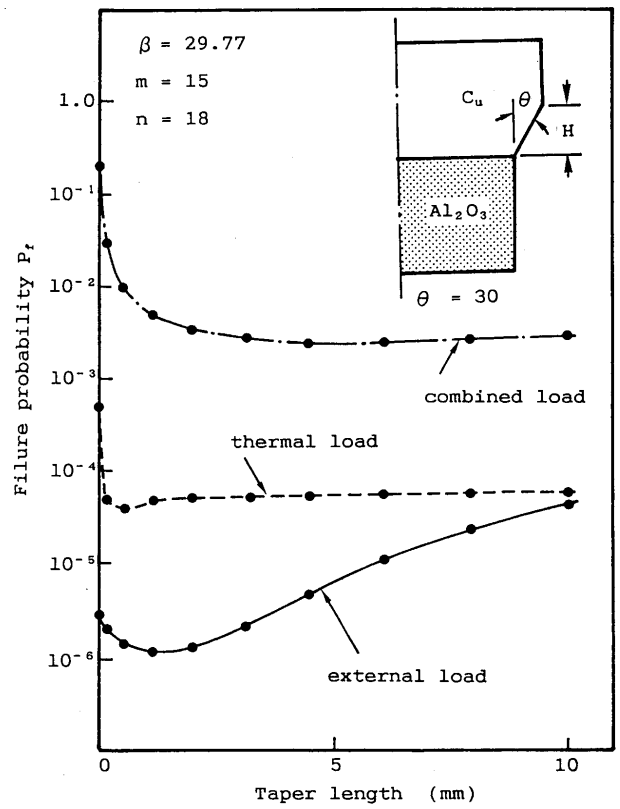


Fig. 15 Effect of the taper length on failure probability (convex type).

- (4) In case of thermal load, the local stress field which is closely related to the singularity is the dominant factor to determine the failure probability and the optimum shape. The macroscopic stress should be also considered when only external load is acting.

Acknowledgements

The authors would like to acknowledge the great help by Mr. Morio Nambu (Student in Faculty of Engineering, Osaka University) in conducting the numerical analyses.

References

- 1) K. Seo, M. Kusaka, F. Nogata, T. Terasaki, Y. Nakao and K. Saida, "Study on the Thermal Stress at Ceramics-Metal Joint", Trans. of Japan Society of Mechanical Engineers Series A, 55-510 (1989 in Japanese), 312-317.
- 2) H. Kobayashi, Y. Arai, H. Nakamura and M. Nakamura, "Mechanics Approach to Fracture Strength of Ceramics/Metal Joints", Trans. of Japan Society of mechanical Engineers Series A, Vol. 55, No. 512 (1989 in Japanese), 750-755.
- 3) H. Koguchi, T. Kaya, Y. Ohtani and T. Yada, "Reliability Evaluation of Joints of Ceramics and Metals (3rd Report, Discussion and comparison for the effect of modification of joints geometry upon the thermal stress concentration by thermoelastic and thermoelastic-plastic analysis)", Trans. of Japan Society of mechanical Engineers Series A, Vol. 55, No. 513 (1989 in Japanese), 1121-1125.
- 4) H. Murakawa and Y. Ueda, "Shape Optimization for Reducing stress at Ceramics/Metal Joints", Trans. JWRI, Vol. 18, No. 2 (1989), 133-140.
- 5) V. L. Hein and F. Erdogan, "Stress Singularities in a Two-Material Wedge", International Journal of Fracture Mechanics, Vol. 7, No. 3 (1971), 317-330.
- 6) H. Murata, Y. Matsuo, M. Miyakawa and K. Kitakami, "Role of Fracture Diagnostic data in Estimation of Parameters for Multimodal Weibull Distribution Function", Trans. of Japan Society of Mechanical Engineers Series A, Vol. 52, No. 473 (1986 in Japanese), 27-34.